Effect of grain refinement on mechanical and corrosion behavior of AZ91 magnesium alloy processed by ECAE

IOP Conf. Series: Materials Science and Engineering **591** (2019) 012015 doi:10.1088/1757-899X/591/1/012015

Effect of grain refinement on mechanical and corrosion behavior of AZ91 magnesium alloy processed by ECAE

M N Gajanan[1], S Narendranath[1] and S S Satheesh Kumar[2]
[1]NITK, Determent of Mechanical Engineering, Surathkal, Mangalore 575025, India
[2]Near Net Shape Group, DMRL, Kanchanbagh, Hyderabad 500058, India

E-mail: gajamnaik@gmail.com

Abstract. AZ91 Mg alloys were processed by equal channel angular extrusion (ECAE) up to 4 passes through route-R. The increase in number of ECAE passes to yield fine-grain structure in the bulk Mg alloy with a more dislocation density, this enhances mechanical properties and corrosion resistance. Indeed, microstructural observations revealed an equiaxed and significant grain refinement after ECAE-4P, with a mean grain size (d) of ~ 4.36µm. Further, the tensile strength, micro-hardness and corrosion resistance were also increased, however the elongation was reduced with the increasing of ECAE passes. The electrochemical polarization test in 3.5wt % NaCl solution revealed a noticeable enhancement in the corrosion resistance of ECAE processed AZ91 Mg alloy compared with the as-received Mg alloy. This is mainly due to grain refinement and distribution of secondary phase particles in Mg alloy matrix during ECAE-4P.

1. Introduction

Ultrafine grain (UFG) magnesium alloys processed by equal channel angular extrusion (ECAE) have been reported to have superior tensile strength with improved ductility at elevated processing temperature [1]. In the last decade, various metals and alloys such as Al, Cu, Ti, steels, including magnesium and its alloys have been effectively extruded by the ECAE. For magnesium alloys, most of the ECAE studies has focused on grain boundary strengthening of AZ Mg alloys. Little attention has been focused to grain boundary strengthening and corrosion resistance of AZ91 Mg alloys. Which are extensively used for automobile, biomedical and chemical industries [2, 3]. Cold working, which commonly improves the tensile strength of metals and alloys, has been found to be unsuccessful in enhancing the strength of AZ Mg alloys due to HCP crystal with the minimum slip system [4]. It is of great attention to exploring the strengthening effect below recrystallization temperature in ECAP in the AZ91 Mg alloys. It is promising to significantly improve the strength and corrosion resistance of AZ91 alloys, making them much more attractive in industrial applications. However, some researchers have reported a grain boundary strengthening of Mg alloys through ECAE. Avvari et al. [5] improved the mechanical properties of AZ31 Mg alloys after processing with ECAP owing to grain refinement. Yuchun et al. [6] achieved high tensile strength and improved ductility in ZK60 Mg alloy by grain refinement and precipitate hardening through the use of annealing treatment and ECAP. Minárik et al. [7] explored the grain refinement through ECAP for LAE442 Mg alloys. The as-cast and ECAPed microstructure consisted of average grain size of ~1 mm and ~1.7 µm respectively. Naik et al [8] studied that the grain size reduction through ECAP and post-ECAP treatment enhances the microhardness of the AZ80 Mg alloy. Gopi et al [9] employed ECAP at below recrystallization

temperature to prepare AM70 alloy with a mean grain size of 1μm, and noticeable improvement in mechanical properties was observed. Muralidhar et al. [10] found that grain refinement through ECAP of AZ80 Mg alloy could result in superior mechanical strength at below recrystallization temperature. Branislav et al. [11] examined the effect of ECAP process on the corrosion performance of an AZ80 alloy. They reported that grain refinement improves the electrochemical corrosion behaviour of Mg alloys indicating improved passivity. Similarly, Ehsan et al. [12] have also stated thermo-mechanical treatment through ECAE decreases the grain size and the size of the secondary phase particles as a result improving microstructure uniformity, thereby reducing the pitting corrosion effects.

Accordingly, AZ91 Mg alloys were extruded by ECAE. The microstructural evolution of samples was analysed by Optical microscopy (OM), scanning electron microscope (SEM), and X-ray diffraction (XRD). The mechanical properties of extruded samples were evaluated by microhardness and tensile testing. Further, the corrosion resistance of ECAPed Mg alloys was measured. Furthermore, the effect of grain boundary strengthening mechanism-particularly for grain refinement and secondary phase strengthening was evidently discussed.

2. Materials and Experimental work

Commercially available AZ91 Mg alloy (Al-9wt%, Zn-0.5wt%, Mg-Bal.) was supplied by Exclusive Magnesium Pvt Ltd, Hyderabad, India with an initial diameter of 20mm and 200mm length. All rods of AZ91 alloy were machined to diameter of 16mm, length 80mm and the rods were then homogenized for 24h at 400°C.

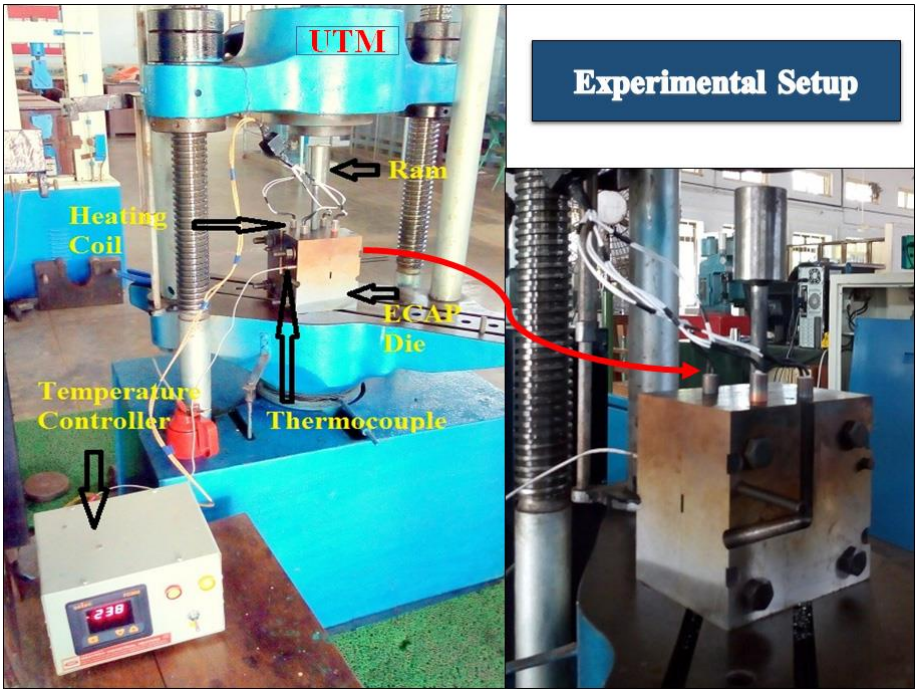

Figure 1. Equal channel angular extrusion experimental setup.

Then, all samples were extruded using an ECAE die having a channel angle 90º and with a corner angle 30°; the schematic of ECAE facility is illustrated in figure 1. Mg alloys processed by the ECAE to a maximum equivalent plastic strain of 4 [13] by four passes (4P) following route R [14]. Molybdenum disulphide (MoS_2) high-temperature grease was used as a lubricant. Pressing of AZ91 alloy was accomplished at 260ºC at the ram speed of 1mm/s for all ECAE passes. The microstructure and morphology of samples were characterized by optical microscopy (OM), Scanning electron microscopy (SEM- JEO JSM–638OLA from JEOL, USA) respectively. Tensile samples were machined with a gauge

length of 16mm and a diameter of 4mm (ASTM E8), the tests were accomplished with a Shimadzu universal testing machine at room temperature. Microhardness tester was operated at load of 100g and dwell time is 13s. X-ray diffraction (Model: PROTO– iXRD MGR40 from Proto Manufacturing Ltd., CANADA) was carried out by an angle range of 2θ: 20º - 90º and a scan speed of 20º/min. The corrosion properties of ECAPed AZ91 Mg alloys were examined by electrochemical corrosion analyzer; Model: Gill AC-1684. The potentiodynamic polarization was performed in 3.5wt% NaCl solution. The auxiliary electrode (AE) was made of graphite (Gr) and the reference electrode (RE) was made of a saturated calomel electrode (SCE) and 1cm^2 area of the working electrode (AZ91 alloy). Potentiodynamic polarization tests were conducted using a scan range of -200mV to +200mV and a scan rate of 2mV/s.

3. Results and discussion

3.1. Microstructure Analysis

Figure 2 presents the optical images of the as-received and ECAPed AZ91 Mg alloy samples. The microstructure of the as-received AZ91 Mg alloy shows a coarse α-Mg phase and β-$Mg_{17}Al_{12}$ secondary phase along the grain boundaries which is confirmed through XRD analysis as shown in figure 4. The mean grain size of the as-received Mg alloy was ~58.69µm, measured by linear intercept method (ASTM E 112). From figure 2(a) it is observed that microstructure was commonly inhomogeneous and there were coarse grains. Further, grains were reduced to the mean size of ~30.52 µm, 4.36 µm after two and four ECAE passes at 533 K respectively, as presented in figure 2(b) and (c). After 4 passes, the microstructural consistency improved compared to the 2-pass AZ91 Mg alloy processed at the same processing temperature. Grain refinement is observed at all the ECAE passes, it is believed that dynamic recrystallization (DRX) occurred during ECAE [15]. Apparently, bimodal grain distributions where coarse grains are enclosed by groups of DRXed grains were observed on ECAP-2P samples. Further increase of ECAP passes a significant reduction in the bimodal microstructure of grain refinement were recorded. A related observation was made on Mg alloys by Roberto et al. [16]. Also, the grain refinement causes the density of grain boundary increase, which increases the hindrance for dislocation movement contributes to the improved mechanical properties of as-received AZ91 alloy [8].

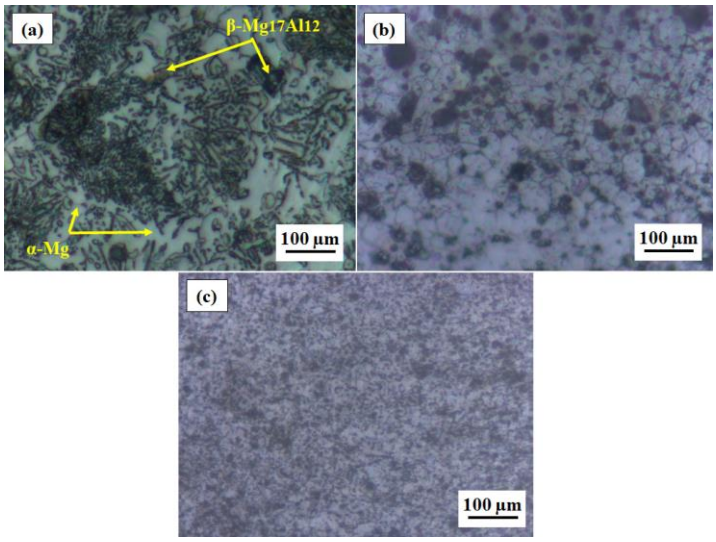

Figure 2. Optical images of AZ91 Mg alloys (a) As-received (b) 2P (c) 4P.

Further, microstructure observation was carried out on the ECAP-4P sample provides direct evidence of the distribution of $Mg_{17}Al_{12}$ in the Mg matrix. A distribution was present after the ECAP-4P as shown in figure 3 which was confirmed through the EDS results. The X-ray diffraction patterns

of as-received and ECAE-4P alloys are shown in figure 4. XRD results suggest that the main phases are α-Mg matrix, β-$Mg_{17}Al_{12}$. The peak intensity of ECAPed AZ91 Mg alloy was reduced when compared to as-received alloys, this is mainly due to grain refinement during ECAE.

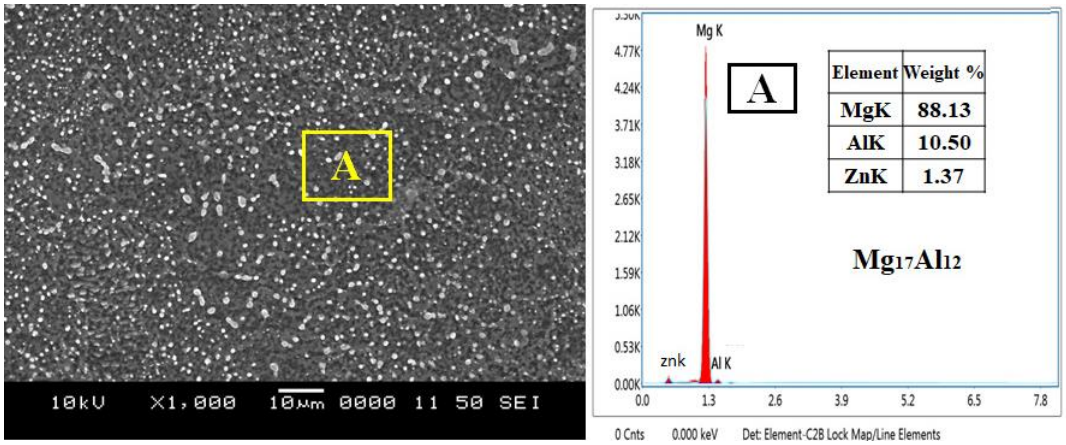

Figure 3. Distribution of secondary phase after ECAP-4P with EDS result.

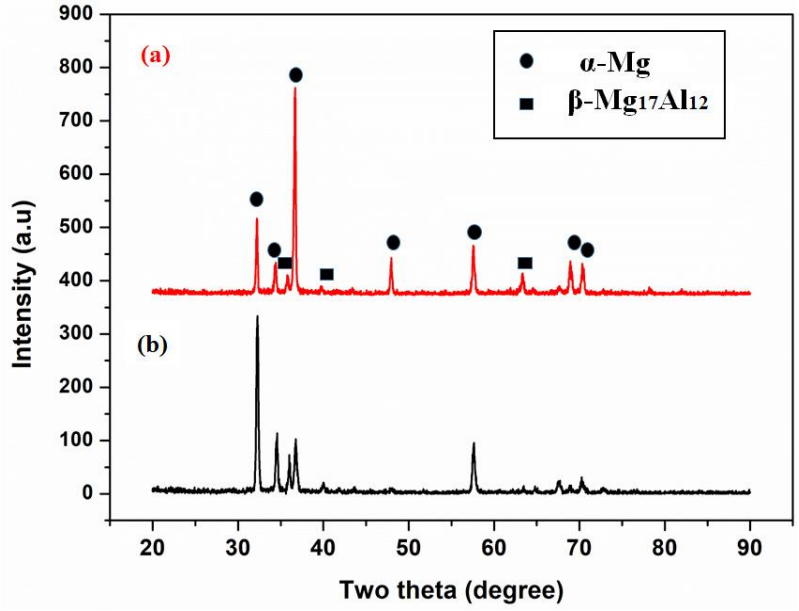

Figure 4. X-Ray diffraction peaks of AZ91 Mg alloys a) As-received b) 4P.

3.2. Mechanical Properties

The microhardness and tensile properties of AZ91 Mg alloy were evaluated after processing by ECAE for 2, 4 passes and presented in figure 5. Figure 5(a) presented the microhardness of the tested Mg alloys. It is evident that the microhardness increasing with respect to ECAP passes and also maximum microhardness of Alloy processed after 4 ECAP passes showed 90 Hv, which is 25% higher than that of as-received AZ91 alloy. The increased microhardness mainly results from the sum of the effects of grain refinement and β-$Mg_{17}Al_{12}$ phase fragmentation, partial dissolution and distribution, which is evidently shown from figures 2 and 3. Engineering stress-strain curves of AZ91 Mg alloys were shown in figure 5(b). Apparently, the yield strength (YS), ultimate tensile strength (UTS) and % elongation were improved after ECAE processing compared with the as-received alloy. However, simultaneous growth in both tensile strength and % elongation with an increasing number of ECAP passes were observed, this enhancement is mainly due to

grain refinement [17]. In addition, 2P and 4P samples achieved higher ductility and ultimate tensile strength respectively. It is reported that after 4P of ECAE the percentage increase of UTS and elongation is 19% and 34% respectively, which is higher than that of the as-received Mg alloy. Similarly, Xia et al. [18] observed the continuous improvement in hardness, tensile strength and ductility of the AZ31 Mg alloy during ECAP. As a comparison, the engineering stress-strain curves for ECAP-2P and ECAP-4P are shown in figure 5(b). From figure 5(b), it is disclosed that after ECAE, the YS and UTS increased noticeably. However, the % elongation of material decreases, this result would be affected by the refinement of grain size. The SEM fractography of as-received and ECAPed samples are reported in figure 6. The fractured surfaces of the as-received, ECAP-2P and 4P sample at room temperature are shown in figures 6(a)-(c) respectively. Figure 6(a) discloses cleavage fracture result in brittle fracture due to coarse grain size. Whereas the ECAPed fractured sample showed mixed mode fracture with cleavage and dimpled features on the fractured surface. Mainly fine and dense dimples with few cleavages depicted in figures 6(b) and (c), indicating a quasi-cleavage fracture, this is mainly initiated by the uniform distribution of fine brittle secondary phase during ECAE [19].

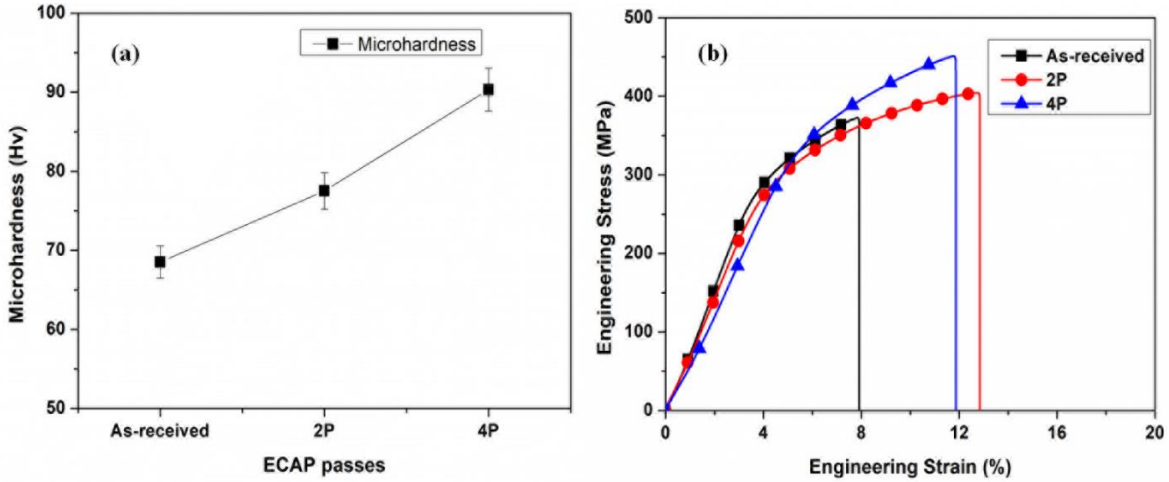

Figure 5. Mechanical properties of AZ91 Mg alloys a) Microhardness b) Engineering stress strain curves.

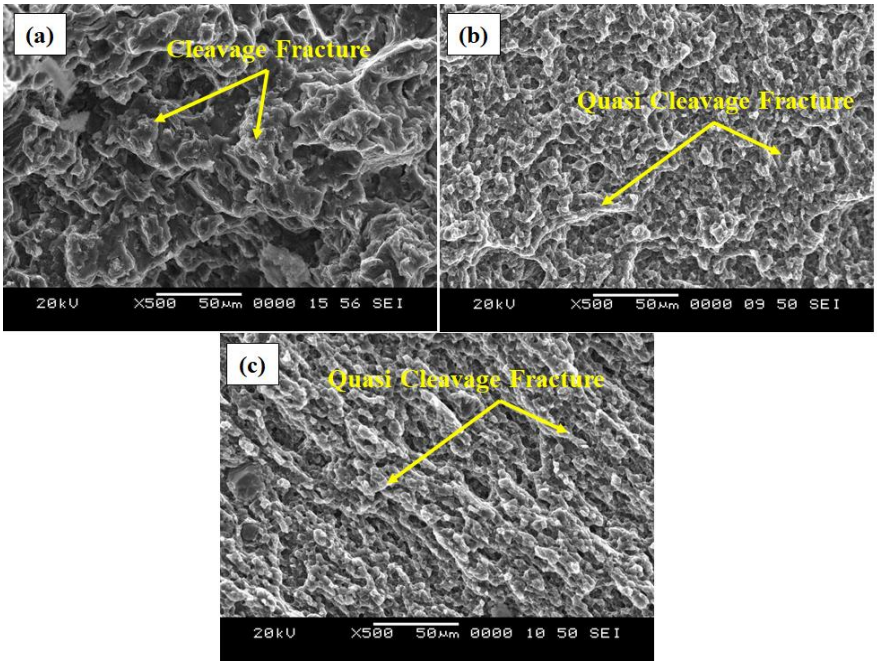

Figure 6. Fractography of AZ91 Mg alloys (a) As-received (b) 2P (c) 4P.

3.3. Corrosion behaviour

The potentiodynamic polarization curves of as-received and ECAPed AZ91 Mg specimens in 3.5wt.% NaCl is shown in figure 7. The experimental results revealed that the Ecorr, corrosion potential of 4P-ECAPed AZ91 Mg alloys was $-1.453V_{SCE}$, which was less negative compared with the as-received alloy (figure 7). This phenomenon specifies that the cathodic reaction was more difficult in fine-grained Mg alloys compared to the coarse grain alloy. Therefore, with the ECAP, the corrosion potential (Ecorr) shifted to $-1.536V_{SCE}$ and $-1.453V_{SCE}$ after two and four ECAP passes which are considerably nobler in comparison with the as-received alloy ($-1.540V_{SCE}$). However, the corrosion potential increases with the grain refinement after ECAE in the alloy. Also, the corrosion current density (icorr) of 2P and 4P ECAPed AZ91 Mg alloy was 0.0173mA/cm^2 and 0.0053mA/cm^2 respectively, which is lesser than that of as-received AZ91 Mg alloy (0.0263 mA/cm^2). The obtained results revealed that the ECAPed Mg sample after 4 passes has nobler corrosion potential and lower current density when compared with as-received and ECAPed-2P. Therefore, ECAE increased the corrosion resistance of Mg alloy this is due to grain refinement and distribution of secondary phases [20]. Which is evidently shown in OM and SEM microstructure in figures 2 and 3. Similarly, Shahar et al. [21] explored that the grain refinement and secondary phase distribution through ECAP improves the corrosion resistance of Mg alloys.

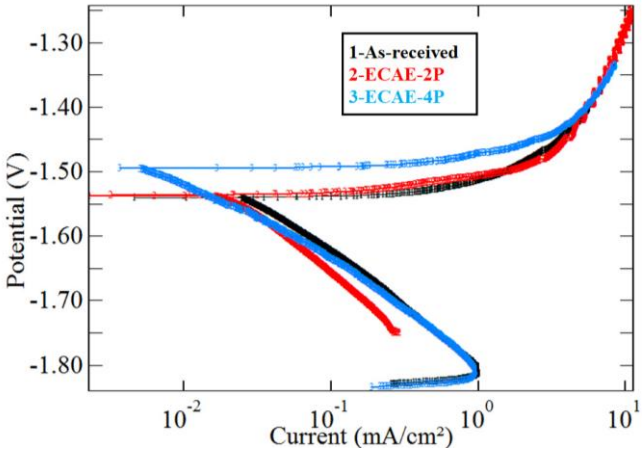

Figure 7. Polarization curves of ECAPed AZ91 Mg alloys.

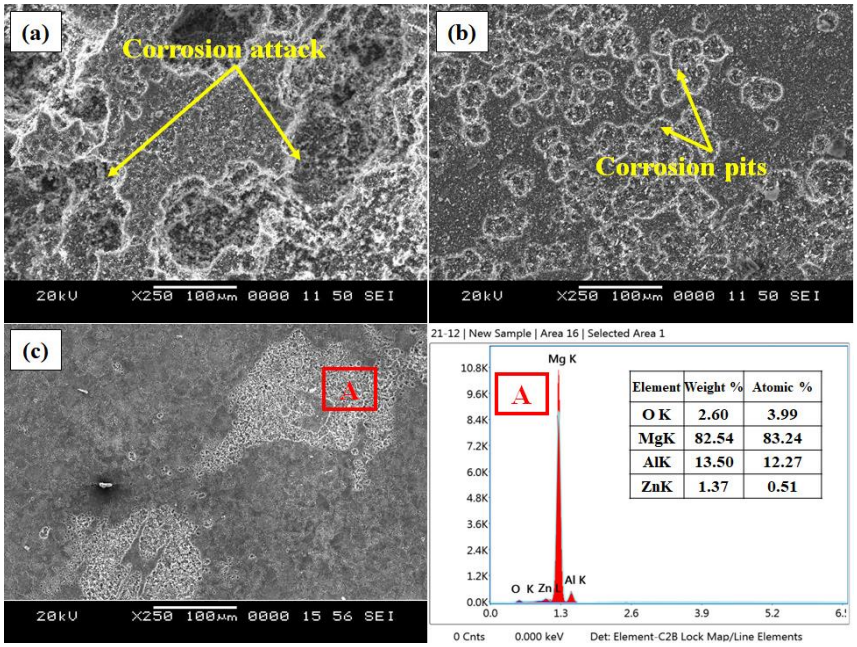

Figure 8. Corrosion morphology for (a) As-received (b) 2P (c) 4P with EDS result.

Figure 8 (a)-(c) shows the surface morphologies of the corroded surface and the corresponding EDS analysis of AZ91 Mg alloys in 3.5wt% NaCl solution. The surface of AZ91 alloy has been shielded by insoluble corrosion products Mg $(OH)_2$ which is confirmed from EDS result as shown in figure 8(d). From figure 8 it is observed that compared to as-received sample, the corrosion attack on ECAPed specimen is remarkably less. This indicates that decreasing the grain size of Mg alloy, the passivity of AZ91 alloy improves. Song et al. [22] also suggest that the corrosion-product layer is more protective after grain refinement through ECAP.

4. Conclusions

Fine-grain AZ91 Mg alloys were extruded via ECAE processing at 533 K. The increase in processing passes is favourable to the grain refinement, resulting in the improvement of ultimate tensile strength, % elongation and corrosion resistance.

The microhardness of AZ91 Mg alloy with 4 ECAE passes has the maximum value of 90 Hv, with the maximum ultimate tensile strength of 455MPa and elongation of 12.6%, respectively. The UTS of 4P-ECAPed AZ91 Mg alloy increased by 19% and percentage elongation of 2P-ECAPed Mg alloys increased by 38% compared to as-received alloy.

The fine-grain AZ91Mg alloy has marginally higher corrosion resistance than the as-received AZ91 with coarser grains, particularly 80% enhancement of corrosion resistance was observed for 4P-ECAP sample.

5. References

[1] Alaneme K K and Okotete E A 2017 *J. magnesium and alloys* **5** 460-475
[2] Zhao L, Ma G, Jin P, Li X and Yu Z 2018*Mater. Res. Express* **6** 036-524
[3] Barnett M R, Nave M D and Bettles C J 2004 *Mater. Sci. Eng. A* **386** 205-211
[4] Naik G M, Gote G D, Narendranath S and Kumar S 2018 *Mater. Res. Express* **5** 086513
[5] Muralidhar A, Narendranath S and Nayaka H S 2013 *J. Magnesium and Alloys* **1** 336-340
[6] Yuan Y, Ma A, Gou X, Jiang J, Arhin G, Song D, Liu H 2016 *Mater. Sci. Eng. A* **677** 125-132
[7] Minarik P, Kral R, Pesicka J, Danis S and Janecek M 2016 *Mater. Chara.* **112** 1-10
[8] Naik G M, Gote G D and Narendranath S 2018 *Mater. today: Proc.* **5** 17763-17768
[9] Gopi K R, Nayaka H S and Sahu S 2016 *J. Mater. Eng. Perfor.* **25** 3737-3745
[10] Avvari M. and Narendranath S 2018 *Silicon* **10** 39-47
[11] Hadzima B, Janecek M, Suchy P, Muller Wagner L 2008 *Mater. Sci. Forum* **584** 994-999
[12] Mostaed E, Vedani M, Hashempour M and Bestetti M 2014 *Biomatter* **4** 28283
[13] Djavanroodi O and Ebrahimi S M 2012 *Prog. Nat. sci.: Mater. Int.* **22** 452-460
[14] Avvari M and Narendranath S 2014 *J.Magnesium and Alloys* **2** 159-164
[15] Jiang Xu C, Yan Lu S H, Nakata T, Lao C S and Han E 2018 *Scientific reports* **8** 16800
[16] Figueiredo R B and Langdon T G 2009 *J. mater. Sci.* **44** 4758-4762
[17] Lin J, Ren W, Wang Q, Ma L and Chen Y 2014 *Adv. Mater. Sci. Eng.* 1-9
[18] Xia K, Wang J T, Wu X, Chen G and Gurvan M 2005 *Mater. Sci. Eng.: A* **410** 324-327
[19] Yakubtsov I, Diak B, Bhattacharya B, MacDonald W, Niewczas M 2008 *Mater. Sci. Eng.: A* **496** 247-255
[20] Gajanan M N, Narendranath S and Satheesh Kumar SS 2019 *AIP Conf. Proc*. **2082** 030016
[21] Shahar I A, Hosaka T, Yoshihara S and Macdonald B. J 2017 *Proc. Eng.* **184** 423-431
[22] Song D, Li C, Liang N, Yang F, Jiang J, Sun J and Ma X *Mater. Des.* 107621

Acknowledgment

This work was supported by DRDO-NRB, Government of India, under grant number NRB/4003/PG/366.